

Densification and metamorphism of new snow

S. Schleef et al.

This discussion paper is/has been under review for the journal The Cryosphere (TC).
Please refer to the corresponding final paper in TC if available.

Influence of stress, temperature and crystal habit on isothermal densification and specific surface area decrease of new snow

S. Schleef, H. Löwe, and M. Schneebeli

WSL Institute for Snow and Avalanche Research SLF, Davos, Switzerland

Received: 10 February 2014 – Accepted: 16 March 2014 – Published: 31 March 2014

Correspondence to: H. Löwe (loewe@slf.ch)

Published by Copernicus Publications on behalf of the European Geosciences Union.

Title Page

Abstract

Introduction

Conclusions

References

Tables

Figures



Back

Close

Full Screen / Esc

Printer-friendly Version

Interactive Discussion



Abstract

Laboratory-based, experimental data for the microstructural evolution of new snow is scarce, though applications would benefit from a quantitative characterization of the main mechanism underlying the initial microstructural changes. To this end we have analyzed the metamorphism and concurrent densification of new snow under isothermal conditions by means of X-ray microtomography and compiled a comprehensive data set of 45 time series covering the practically relevant short time behavior within the first 24–48 h in high temporal resolution. The data set comprises natural and laboratory grown snow and experimental conditions include systematic variations of overburden stress, temperature and crystal habit to address the main influences on specific surface area (SSA) decrease rate and densification rate in a natural snowpack. For all conditions we find a linear increase of the density with the SSA, indicating that metamorphism has a key influence for the densification of new snow. Corroborated by the analysis of the individual influences of external conditions we derive a best-fit parametrization for the SSA decrease rate and the densification rate as required for applications.

1 Introduction

The temporal evolution of new snow is delicate, since fast changes of bulk density or specific surface area (SSA) as key microstructural characteristics occur shortly within hours after snowfall. Various applications rely on a quantitative understanding of these initial snowpack processes. For avalanche prediction a fast or slowly densifying snowpack eventually discerns between conditions of high or low snowpack stability and initial modeling uncertainties of the densification density will propagate and persist through the entire season (Steinkogler et al., 2009). The density of snow is also important for hydrological applications where estimates of snow water equivalent are commonly obtained from snow height measurements of meteorological stations via empirical cor-

TCD

8, 1795–1829, 2014

Densification and metamorphism of new snow

S. Schleef et al.

Title Page

Abstract

Introduction

Conclusions

References

Tables

Figures

◀

▶

◀

▶

Back

Close

Full Screen / Esc

Printer-friendly Version

Interactive Discussion



relations between height and density. The development of these parametrizations is complicated by intermediate snow falls and its short time evolution during subsequent densification (McCreight and Small, 2013). If the state of the snowpack is instead monitored via remote sensing, the key quantity is snow albedo which is mainly determined via SSA (Flanner and Zender, 2006) and even thin layers of new snow have a measurable impact on the total snow albedo (Perovich, 2007). Finally, the validation of winter precipitation schemes for meteorological models also rely on the connection between airborne crystal sizes (which might be related to the inverse SSA) and the bulk densities of new snow (Thompson et al., 2008).

From a modeling perspective the evolution of new snow on the ground can be addressed by snowpack models which primarily aim at a description of densification rates in terms of overburden and temperature (Jordan, 1991; Lehning et al., 2002; Vionnet et al., 2012). Some of these models also include the microstructure in terms of empirical parameters such as grain size, dendricity and sphericity. These parameters are however ambiguous to be determined objectively and recent versions of snowpack models aim at replacing grain size by the optical radius (or inverse specific surface area) (Carmagnola et al., 2013) which can be measured objectively by various techniques in the field. Validations of the new model rely on experimental data for the density and the specific surface area, which can be considered as the most important microstructural parameters for the aforementioned models.

Previously, some progress has been made to understand the physical mechanisms underlying new snow densification and metamorphism within creep experiments (Schleef and Löwe, 2013). The results indicate that the evolution of the SSA occurs rather autonomously without being affected by the concurrent densification. The experiments were carried out for a single type of nature-identical new snow at a single temperature. This small range of experimental conditions is however of only limited, direct use for the aforementioned applications. To cover a wide range of natural conditions for snow types and temperatures, applications are naturally interested in best fit behavior of large data sets which are essential benchmarks to validate and drive snow

Densification and metamorphism of new snow

S. Schleef et al.

[Title Page](#)[Abstract](#)[Introduction](#)[Conclusions](#)[References](#)[Tables](#)[Figures](#)[Back](#)[Close](#)[Full Screen / Esc](#)[Printer-friendly Version](#)[Interactive Discussion](#)

evolution models. Data sets are available for well-aged seasonal snow (Dominé et al., 2007) and data of experiments which includes new snow at the beginning (Cabanes et al., 2002, 2003; Legagneux et al., 2003; Taillandier et al., 2007). But comparable data from in-situ experiments which monitor the evolution of the *same* sample of new snow at high temporal resolution is almost non-existent.

To fill this gap we present a comprehensive data set of tomography experiments for new snow densification and metamorphism covering various examples of natural and laboratory-grown new snow with a wide range of crystal habits. By carrying out in-situ creep experiments at different temperatures and overburden stresses, the evolution of the main microstructural parameters, the ice volume fraction ϕ_{ice} and the SSA, is monitored typically over one to two days at a temporal resolution of 3 h. A reference experiment over an entire week indicates that this is sufficient to capture the main aspects of microstructural changes. As a generic result for all parameters, we consistently find an almost linear relation between the density and the specific surface area. Based on this observation and previous modeling ideas for the SSA and densification rate we present simple parametrizations for the microstructural evolution of new snow in terms of the most important parameters for snow models namely ϕ_{ice} , SSA, temperature T and stress σ . The influence of these parameters are discussed separately. To understand particularities of the results we also analyzed the Euler characteristic as an additional parameter, which was recently employed to interpret compression experiments of new snow (Schleef et al., 2014b).

2 Methods

For the following isothermal tomography measurements and their analysis we refer to Schleef and Löwe (2013) for an elaborate description of the experimental details. For a self-contained presentation we summarize the main steps of the method and outline differences or extensions to Schleef and Löwe (2013).

Densification and metamorphism of new snow

S. Schleef et al.

Title Page

Abstract

Introduction

Conclusions

References

Tables

Figures



Back

Close

Full Screen / Esc

Printer-friendly Version

Interactive Discussion



Densification and metamorphism of new snow

S. Schlee et al.

Title Page

Abstract

Introduction

Conclusions

References

Tables

Figures

◀

▶

◀

▶

Back

Close

Full Screen / Esc

Printer-friendly Version

Interactive Discussion



All snow samples were prepared from fresh snow, which was either collected outside or produced with a machine in the cold laboratory (Schlee et al., 2014a). An overview of all sets of experiments with their main characteristics is given in Table 1. The natural snow was collected just outside the cold laboratory in Davos, Switzerland, during the winters 2011/2012 and 2012/2013. Only intense snowfalls at air temperatures below -2°C with a deposition time less than an hour were chosen to minimize previous metamorphism. Immediately afterwards the snow was sieved (mesh size 1 mm) into sample holders of 18 mm diameter with 15 mm filling height. In between, photographs of sieved snow crystals were taken to capture the crystal habit. Each set of snow samples comprised several identically prepared samples which were stored in a freezer at -60°C to nearly suppresses metamorphism until the experiments (Kaempfer and Schneebeli, 2007). In total, 8 sets of snow samples from different natural snow falls and 6 sets from different snowmaker runs were prepared which are listed in Table 1.

The experiments were conducted within at most 3 weeks after sample preparation. The respective sample was placed in the cold laboratory one hour before the first measurement for thermal equilibration. For some experiments (Table 1) a cylindrical weight of 133, 215 or 318 Pa was carefully put on the sample half an hour before starting the first measurement to analyze the influence of external stress. Stress values were chosen to mimic different potential bury depths of new snow inside the snowpack, the stress values correspond to bury depths of about 0–30 cm, given an average new snow density of 100 kg m^{-3} .

The measurements were conducted with a desktop computer tomograph (μCT 80, SCANCO medical) operated in a cold laboratory at isothermal temperatures of about -13 or -18°C . For a single set (no. 14, cf. Table 1) the temperature was varied systematically to higher values of about -3 and -8°C to investigate the influence of temperature. For these samples the temperature was recorded during the whole experiment with a sensor (iButton device) in the sealing cap of the sample holder. All samples were kept undisturbed in the μCT during the whole experiment which took one or two days. In one case the measurement was extended to an entire week. μCT scans of a fixed

volume of 6.3 mm height in the middle of the samples were conducted automatically with a time-interval of 3 h. The nominal resolution was 10 μm voxel size and the energy 45 kV. One scan took about two hours. In total, 45 time series were measured leading to more than 600 μCT scans.

For the analysis a cubic volume of 6.3 mm edge length was extracted for each measurement and segmented into a binary file of ice and air. From the resulting 3-D images the ice fraction and the specific surface area was calculated (details in Schleef and Löwe, 2013). In the following the results are exclusively presented in terms of the ice volume fraction ϕ_{ice} which is directly obtained from the μCT . The volume fraction can be related to the snow density via $\rho = \phi_{\text{ice}} \rho_{\text{ice}}$ with the temperature dependent density of ice $\rho_{\text{ice}} = 917\text{--}920 \text{ kg m}^{-3}$ (0 to -20°C) (Petrenko and Whitworth, 1999). For the SSA we use the definition as surface area per ice volume, which is related to the surface area per ice mass (SSA_m) by $\text{SSA} = \rho_{\text{ice}} \text{SSA}_m$.

Though we mainly focus on the ice volume fraction and the SSA for the analysis we have additionally evaluated the Euler characteristic χ of the samples. The Euler characteristic provides information about the topology of the samples which has been proven useful to understand the evolution of the snow microstructure under forced compression in a microcompression device (Schleef et al., 2014b). The Euler characteristic $\chi = 2 - 2g$ is related to the interface genus g which is an indicator for the connectivity of a structure (Michelsen et al., 2003). The Euler characteristic typically assumes negative values, corresponding to high positive values of the interface genus. The higher the genus, the lower χ and the higher the number of interparticle contacts. We calculated the Euler characteristic from the integral geometric approach of Minkowski functionals outlined by Michelsen et al. (2003). In accordance to the calculation of the SSA as a surface area per *ice volume* we normalized the Euler characteristic χ by the ice volume.

Densification and metamorphism of new snow

S. Schleef et al.

Title Page

Abstract

Introduction

Conclusions

References

Tables

Figures

◀

▶

◀

▶

Back

Close

Full Screen / Esc

Printer-friendly Version

Interactive Discussion



3 Results

3.1 Overview

The natural new snow samples showed a high variability of their initial characteristics. The nature-identical samples also varied in their initial characteristics and parameters due to different settings of the snowmaker (Schleef et al., 2014a). Overall, the initial ice volume fractions ranged from about 0.05 to 0.12, the initial SSA values were in the range 62–105 mm⁻¹, and the initial χ values were between -2×10^5 mm⁻³ and -12×10^5 mm⁻³. The averaged initial values of ϕ_{ice} and SSA of each new snow type are listed in Table 1. The initial values had an influence on the settling, yielding a faster densification for a lower initial ϕ_{ice} and a faster SSA decay for a higher initial SSA, but also variations of other parameters like temperature and stress led to a high variability. As a starting point for our subsequent analysis we demonstrate the variability in the bare evolution of the ice volume fraction and the SSA for all samples in Figs. 1 and 2, respectively.

For one randomly selected sample of natural snow at -13°C we extended the observation to a whole week. From the analysis we obtained the evolution of ϕ_{ice} and SSA at high temporal resolution, as shown in Fig. 3. For the given example, no external stress was applied, but the volume fraction ϕ_{ice} increased by more than 40% from an initial value of about 0.11. At the same time the SSA decreased from 77 mm⁻¹ to 45 mm⁻¹. A widely confirmed decay law for the SSA (Legagneux et al., 2004; Flanner and Zender, 2006; Kaempfer and Schneebeli, 2007; Schleef and Löwe, 2013) is given by

$$\text{SSA}(t) = \text{SSA}(0) \left(\frac{\tau}{t + \tau} \right)^{1/n} \quad (1)$$

with the parameters τ and n . A fit to the SSA data is shown in Fig. 3 with the parameters $\tau = 27$ h and $n = 3.8$ ($R^2 > 0.99$).

Title Page

Abstract

Introduction

Conclusions

References

Tables

Figures

◀

▶

◀

▶

Back

Close

Full Screen / Esc

Printer-friendly Version

Interactive Discussion



Densification and metamorphism of new snow

S. Schleef et al.

Title Page

Abstract

Introduction

Conclusions

References

Tables

Figures

◀

▶

◀

▶

Back

Close

Full Screen / Esc

Printer-friendly Version

Interactive Discussion



For a visual demonstration of the microstructural evolution we combined sections of the 3-D images to a time-lapse movie which is provided as Supplement. The densification and coarsening is clearly visible in the movie and occurs in the absence of recognizable particle rearrangements and the creation of new interparticle contacts.

This is confirmed by the evolution of the Euler characteristic χ which increases monotonically with a decreasing rate. This behavior of the Euler characteristic is common for most experiments and expected for isothermal coarsening (Kwon et al., 2007). This topological signature of coarsening is not even influenced in the presence of applied stresses. Some examples for the evolution of χ in one day are shown in Fig. 4. For later reference we note that a few samples show a non-monotonic behavior of the Euler characteristic at the beginning of the experiment.

3.2 General relation between density and SSA

Despite the apparent variability of individual curves of density and SSA shown in the previous section, the evolution turns out to be governed by a generic feature. As suggested by Fig. 3 the increase of the volume fraction ϕ_{ice} seems to “mirror” the SSA decay. If the ice volume fraction ϕ_{ice} is plotted vs. the SSA for all series (Fig. 5) an almost linear relation between both is consistently revealed irrespective of the experimental conditions. Except for one sample, which showed no densification at all, all other series of measurements can be fitted to an empirical linear relation $\phi_{\text{ice}} = a \cdot \text{SSA} + b$ with coefficient of variation $R^2 > 0.94$. The fit parameters vary in the range $a = [-2 \times 10^{-3}, -0.2 \times 10^{-3}]$ and $b = [0.08, 0.26]$ depending on applied stresses, temperatures or crystal habits, however, not in an apparent systematic way as shown in Fig. 5. We note that likewise a logarithmic law $\ln(\phi_{\text{ice}}) = a' \cdot \text{SSA} + b'$ could be fitted to the data, with values $a' = [-2 \times 10^{-2}, -0.3 \times 10^{-2}]$ and $b' = [-2.5, -0.4]$ and $R^2 > 0.93$. This logarithmic dependence was suggested by Legagneux et al. (2002); Dominé et al. (2007). The difficulty of discerning a logarithmic from a linear relation is not surprising since $\ln(x) \approx -1 + x$ for values x close to one where both models seem to be equally

valid. A detailed analysis of the experimental parameters on the SSA evolution and the densification will be carried out below.

3.3 Influence of temperature

To investigate the influence of different (isothermal) temperatures we measured the settling for one set of samples (snow 9 in Table 1) at 3 different laboratory temperatures. The temperature of the samples was recorded continuously during the experiments resulting in mean values of -3.1°C , -8.3°C and -13.4°C . Even though additional fans are mounted inside the μCT to minimize temperature fluctuations, the temperature changed during each scan by up to $\pm 0.5^{\circ}\text{C}$ due to the heating of the X-ray tube. In addition, the defrosting cycles of the cold laboratory heat exchanger caused small changes of the temperature twice a day. In total, the temperature fluctuations were at maximum $\pm 0.6^{\circ}\text{C}$ during one day, with the highest changes for the mean temperature of -3.1°C . For each temperature, we conducted one series without a weight on the sample and another one with a weight corresponding to a stress of 133 Pa and analyzed the density and the SSA.

3.3.1 Densification rate

The initial ice fractions of the samples were about 0.06–0.09. For the samples without applied stress almost no densification was observed within one day. Therefore a clear dependency on the temperature could not be obtained from the data of these samples. In contrast, the series with an applied stress of 133 Pa showed a significant, steady densification of 27–48 % per day which is clearly influenced by the temperature. The temperature influence of the densification of snow is often described by an Arrhenius law (Bader, 1960; Arnaud et al., 2000; Kirchner et al., 2001; Delmas, 2013)

$$\dot{\phi}_{\text{ice}}/\phi_{\text{ice}} = v \exp\left(-\frac{E}{k_{\text{B}}T_{\text{K}}}\right) \quad (2)$$

with a rate constant ν , an activation energy E , the Boltzmann constant k_B and the temperature T_K in Kelvin. From the differences of the ice volume fraction between successive time steps we obtain the experimental densification rates. Following the Arrhenius law, the mean densification rates per hour for each series are plotted against the inverse temperature in Kelvin in Fig. 6. The horizontal error bars result from the measured temperature fluctuations whereas the vertical errors bars indicate the maximum deviations from the mean values. By fitting the results to Eq. (2) we find the parameters $\nu = 4.8 \times 10^8 \text{ h}^{-1}$ and $E = 0.56 \text{ eV}$ ($R^2 = 0.49$) for the experiments with a stress of 133 Pa. The same fit for the experiments without stress yields $\nu = 2.8 \text{ h}^{-1}$ and $E = 0.16 \text{ eV}$ ($R^2 = 0.99$), however, there was only marginal change of the density.

3.3.2 SSA decrease rate

The initial SSA of the samples was between 70–78 mm^{-1} . For all samples a steady decay of 12–31 % in one day could be measured. Figure 7 shows the mean SSA decay per hour with error bars calculated in the same way as described for the ice fraction evolution. The SSA decay increased significantly with higher temperatures. At a temperature of about -13°C the decay was almost independent of the applied stress. In contrast, for higher temperatures the experiments with a stress of 133 Pa showed an accelerated rate of SSA decay. The temperature influence can be best described with an empirical linear relation $\text{SSA} = \alpha T + \beta$ with the parameters $\alpha = -0.02$ and $\beta = -0.62$ ($R^2 > 0.99$) for the experiments with stress $p = 0$, and $\alpha = -0.04$, $\beta = -0.99$ ($R^2 = 0.99$) for $p = 133 \text{ Pa}$. This is valid if the temperature is given in $^\circ\text{C}$ and SSA in units $\text{mm}^{-1} \text{ h}^{-1}$. In Fig. 7 the experiments at higher temperatures and $p = 133 \text{ Pa}$ have a disproportionate error on the SSA rate, which is caused by a much higher SSA difference between the first two measurements of the time series. By neglecting the first measurement, the difference of the SSA rate at high temperatures between the experiments with and without applied stress would only be small.

The particularity of the first time step is partly revealed by the Euler characteristic, which is shown for $T \approx -3^\circ\text{C}$ in Fig. 4. The measurements without applied stress show

Title Page

Abstract

Introduction

Conclusions

References

Tables

Figures



Back

Close

Full Screen / Esc

Printer-friendly Version

Interactive Discussion



a monotonic increase, similar to the evolution of the one week measurement and similar to the results for the other experiments, including those described by Schleef and Löwe (2013). For the samples analyzed here, the rate increased slightly with increasing temperature. The measurement with a stress of 133 Pa however showed a different behavior. Within the first 3 h between the first and the second measurement, the Euler characteristic decreases significantly, corresponding to an increase of the number of interparticle contacts. After that, the connectivity decreased again monotonically (i.e. increase of χ) similar to the evolution of the corresponding experiment without applied stress. The rate was however slightly lower.

3.4 Influence of crystal habit

Finally we turn to differences in the crystal habit, and their possible influence on the settling. From the photographs we could compare the crystal habits of our samples to the classification of natural snow crystals (Kikuchi et al., 2013), as listed in Table 1. In most cases we observed broken parts of the respective crystal types, which are likely caused by the sieving. But also wind can lead to broken crystals in nature, and we could still identify the original crystal for the classification. An unambiguous classification for each snow sample was however not possible, because each sample contained a mixture of different crystals. This was particularly the case for natural snow. For some samples, however, specific crystal habits dominated the shape.

Figure 8 shows two examples of natural snow samples with a photo of the prominent crystal habit and the corresponding μ CT image of the initial structure. The sample at bottom is the one with the evolution shown in Fig. 3 (snow 5 in Table 1), with dominant crystal habit of skeletal columns with scrolls (C3c) and combinations of columns and bullets (A1a). For comparison we picked a sample (top in Fig. 8) which had almost the same initial ice fraction (snow 2 in Table 1) but a different dominating crystal habit (broad branches, P2b). This sample was unique since no densification at all could be measured within two days at -18°C , in contrast to the previous sample (snow 5) which showed a densification of about 18 % in the same time at -13°C . However, the high

Densification and metamorphism of new snow

S. Schleef et al.

Title Page

Abstract

Introduction

Conclusions

References

Tables

Figures



Back

Close

Full Screen / Esc

Printer-friendly Version

Interactive Discussion



experiments (Schleef et al., 2014b). With that we consider that the SSA is not only affected by metamorphism but also by the number of contacts during settling between the ice grains. Crucial topological changes, i.e. the creation of new contacts within the structure, occurred only for a few samples at the beginning of the series of measurements.

A fit of Eq. (4) to the SSA rates obtained from the difference of successive measurement within typically three hours for our complete data set yield $a = 2.9 \times 10^{-7}$, $b = 9.5 \times 10^{-9}$, $c = -3.5 \times 10^{-3}$ and $m = 3.5$ with ($R^2 = 0.83$). This is valid for temperature given in °C, the SSA in units of mm^{-1} and $\dot{\chi}$ in units mm^{-3} . The scatter plot between modeled and measured SSA rates is shown in Fig. 9.

If we neglect the measurements where noticeable topological changes ($\dot{\chi} < 0$) occurred, which was only the case for 10 samples for the first measurements, we could even simplify the model to

$$\dot{\text{SSA}} = (a' + b'T)\text{SSA}^{m'}, \quad (5)$$

leading to fit parameters $a' = 1.1 \times 10^{-6}$, $b' = 3.1 \times 10^{-8}$ and $m' = 3.1$. In this case we obtain an even improved performance ($R^2 = 0.87$). This is particularly interesting, given the practical difficulty to measure the Euler characteristic without tomography.

3.5.2 Densification rate

A parametrization for the densification rate $\dot{\phi}_{\text{ice}}$ for all measurements turns out to be more complicated than for $\dot{\text{SSA}}$, since $\dot{\phi}_{\text{ice}}$ is not only influenced by temperature and the initial value $\phi_{\text{ice},0}$ but also by the stress and the crystal habit, as described before.

To motivate a model which aims to fit the entire data we start from the common stress dependence of the strain rate for visco-plastic flow of polycrystalline ice which is commonly described by Glen's law for secondary creep, $\dot{\epsilon} = A\sigma^k$ (Petrenko and Whitworth, 1999). A similar form is believed to be valid for snow (Kirchner et al., 2001). In a one-dimensional system, the strain rate $\dot{\epsilon}$ can be taken as the relative densification

Densification and metamorphism of new snow

S. Schleef et al.

Title Page

Abstract

Introduction

Conclusions

References

Tables

Figures



Back

Close

Full Screen / Esc

Printer-friendly Version

Interactive Discussion



rate $\dot{\epsilon} = \dot{\phi}/\phi$ (cf. also Schleef and Löwe, 2013) leading to

$$\dot{\phi}_{\text{ice}}/\phi_{\text{ice}} = A\sigma^k \quad (6)$$

with a constant A containing the rate of the process.

On the other hand we have empirically observed that the volume fraction is almost linearly related to the specific surface area. Hence we chose the rate in Eq. (6) to be determined mainly by the SSA rate $A = B\dot{S}SA$ and end up with

$$\dot{\phi}_{\text{ice}}/\phi_{\text{ice}} = B\dot{S}SA\sigma^k \quad (7)$$

for our parametrization model, which includes two parameters B and k . We note that integrating Eq. (7) in fact implies $\ln(\phi_{\text{ice}}) \sim \dot{S}SA$ and not a linear dependence. This is however in accordance with the result from Sect. 3.2 where the logarithmic or the linear relation are indistinguishable. Thus Eq. (7) constitutes a reasonable trade off and naturally includes a dependence of the densification rate on the density itself.

A fit of Eq. (7) to the densification rates obtained from the difference of successive measurements within typically three hours for our complete data set yields $B = -6.6 \times 10^{-3}$ and $k = 0.18$. This is valid for stresses given in units of Pa and $\dot{S}SA$ in units $\text{mm}^{-1} \text{h}^{-1}$. We note that samples without a weight are assigned a remaining, non-zero stress of 5 Pa caused by the small but non-negligible overburden of the overlying snow inside the μCT sample holder on top of the evaluation cube. The same value was chosen by Schleef and Löwe (2013). The scatter plot between modeled and measured densification rates is shown in Fig. 10, yielding $R^2 = 0.82$.

We note that the parametrization Eq. (7) might be slightly improved by including the Euler characteristic via

$$\dot{\phi}_{\text{ice}}/\phi_{\text{ice}} = (B'\sigma^k + C'\dot{\chi})\dot{S}SA \quad (8)$$

which yields $R^2 = 0.85$.

Densification and metamorphism of new snow

S. Schleef et al.

Title Page

Abstract

Introduction

Conclusions

References

Tables

Figures

◀

▶

◀

▶

Back

Close

Full Screen / Esc

Printer-friendly Version

Interactive Discussion



4 Discussion

4.1 Main result

We start the discussion from the parametrization of the SSA and the densification for new snow under isothermal conditions (Sect. 3.5). We note that our experiments focused only on new snow with low density and high SSA and most of our results are probably not valid for denser snow. The parametrizations are motivated by available models for the SSA (Legagneux et al., 2004) and Glen's law for creep of polycrystalline ice (Petrenko and Whitworth, 1999). Most current snowpack models (Vionnet et al., 2012; Jordan, 1991; Bartelt and Lehning, 2002) use a similar approach for the densification, but are based on traditional grain size concerning the microstructure. Recently, the model Crocus was modified to use directly SSA to express the microstructural properties (Carmagnola et al., 2013). In contrast to denser snow under isothermal metamorphism, we found that the densification rate is directly related to metamorphism via the SSA rate. This is reflected by the consistent linear variation of the ice volume fraction with the SSA (Fig. 5). This observation was implemented in the parametrization by a prefactor in the densification rate which is proportional to the SSA rate. We have set up the parametrization for the densification in a way to guarantee that both evolution laws are only dependent on the quantities ϕ_{ice} (or the density), the stress σ , the specific surface area SSA and the temperature T to best fit the entire, available data of new snow. Thereby Eqs. (5) and (7) provide a closed set of empirical, microstructural evolution equations for the density and the SSA under isothermal conditions. Both SSA and density can be obtained in the field, without the use of tomography (Matzl and Schneebeli, 2006; Gallet et al., 2009; Arnaud et al., 2011). The data set provides a comprehensive benchmark to validate new parametrization of snowpack models in terms of SSA and density (Carmagnola et al., 2013). Our new parametrization will also be useful to predict the evolution of the albedo (Flanner and Zender, 2006), as information about the evolution of SSA in new snow is scarce.

Densification and metamorphism of new snow

S. Schleef et al.

Title Page

Abstract

Introduction

Conclusions

References

Tables

Figures



Back

Close

Full Screen / Esc

Printer-friendly Version

Interactive Discussion



4.2 SSA decrease rate

Our simple parametrization for the SSA change Eq. (4) yields good agreement for almost all of our measurement data. The exponent m obtained from the fit must be compared to n from the widely used Eq. (1) via $n = m - 1$, yielding $n = 2.5$. As already outlined by Schlee and Löwe (2013), the precise value of n is difficult to estimate, if the duration of the experiment is similar to τ , which is typically in the order of one day. This is confirmed by the one week measurement which allows a better estimate of the fit parameters in Eq. (1). The obtained exponent $n = 3.8$ agrees well with the results of Legagneux et al. (2004) who found $n = 3.4$ – 5.0 at a temperature of -15°C . In contrast, the results of the short time measurements did not lead to a conclusive estimate for n . Also the fits to the 2 day time series by Schlee and Löwe (2013) gave higher values of n and only an adapted combination of all series resulted to a similar n of about 3.9. However the value $n = 2.5$ indicates that even for short times the SSA decrease rate is dominantly influenced by the present value of the SSA in a non-linear way. It is generally believed that the value of n is also influenced by temperature potentially caused by different underlying mechanisms of mass transport (Vetter et al., 2010; Löwe et al., 2011). In view of the difficulties of estimating n for the short time series we have restricted ourselves to an inclusion of the temperature dependence into the prefactor in Eq. (4) to account for the acceleration of metamorphism at higher temperatures (Fig. 7).

We have previously observed that the SSA evolution is in fact independent of the densification, or respectively the applied stress (Schlee and Löwe, 2013). This is confirmed here for all experiments conducted at about -13°C or -18°C (cf. Table 1) which can thus be generalized to all examined new snow types. Furthermore, in general no difference could be observed between the evolution of sieved natural new snow samples and snowmaker snow, which is in agreement to the results presented by Schlee et al. (2014a).

TCD

8, 1795–1829, 2014

Densification and metamorphism of new snow

S. Schlee et al.

Title Page

Abstract

Introduction

Conclusions

References

Tables

Figures

◀

▶

◀

▶

Back

Close

Full Screen / Esc

Printer-friendly Version

Interactive Discussion



4.3 Densification rate

The analysis of $\dot{\phi}_{\text{ice}}$ is based on the observation of the almost linear relation between the evolution of ϕ_{ice} and SSA for each series of measurement (Fig. 5). Measurements of Legagneux et al. (2002); Dominé et al. (2007) showed a logarithmic relation between density and SSA, which was however derived from independent measurements in a seasonal snowpack and covered much wider SSA and density ranges. As outlined in Sect. 3.2 a logarithmic relation for each of our series of measurement would also be possible here, and the linear relation might only be an approximation for short observation times.

In contrast to the SSA rate, a direct temperature dependence of the densification rate is less pronounced in the overall behavior of the densification rate. This originates from the fact that the main impact of densification comes from metamorphism itself via the SSA rate in Eq. (7), which implicitly contains a temperature dependence as discussed in the previous section. In general we would also expect an explicit temperature dependence for the creep rate A in Eq. (7). The dedicated analysis of the temperature dependence for one of the sets for two stress values (Fig. 6) reveals that the densification is almost negligible for the case without weight. For the experiments with applied stress a faster rate of $\dot{\phi}/\phi$ could only be observed at about -3°C . The Arrhenius fit Eq. (2) yields an activation energy in the same order of magnitude as known for different possible processes in ice (about 1 eV, Kirchner et al., 2001, and references therein), but the limited amount of data with just one series of measurement at -3°C and 133 Pa did not allow for conclusive parameter estimates. Obtaining reliable data for higher temperatures by desktop tomography is generally difficult, since the timescales of the fast structural changes of new snow are already in the order of the scanning intervals. Due to this most experiments were conducted at -13°C or -18°C where no general trend for a faster densification at higher temperatures could be observed.

4.4 Remaining uncertainties

Besides the most important parameters density and SSA we have also calculated the Euler characteristic to provide additional confidence for the interpretation of the results. We have seen that the inclusion of the Euler characteristic in the parametrizations with Eqs. (4) and (8) makes a slight difference for the very initial stage where some particle rearrangements are noticeable. In general we observed for the majority of samples that the Euler characteristic showed a monotonous increase, or equivalently a monotonous decrease of the number of contacts. This is expected from coarsening (Kwon et al., 2007) due to the reduction of finer parts of the structure. For a highly porous material like new snow, the slow creep deformation considered here does not cause significant structural re-arrangements and new contacts. This is confirmed by the visual inspection of the deformation from the movie (cf. Supplement). The inclusion of the topology does not seem to be essential to describe isothermal densification and metamorphism of new snow. Solely for a few experiments we observed an increase of the connectivity at the beginning. This was the case for samples with faster creep rates due to higher temperature, higher stress and/or a very tenuous structure. In this case an influence on the evolution of SSA and ϕ_{ice} can be observed. But in general these initial structural re-arrangements stabilize quickly. This is consistent with the mechanism of externally forced re-arrangements in deformation controlled compression experiments (Schleef et al., 2014b), in a less pronounced way, though.

Another origin of scatter of the model is revealed by the two (out of 584) Δ SSA outliers in Fig. 9. These are the first values of the series of measurements with an applied stress of 133 Pa at temperatures of -3°C and -8°C . Exactly for these measurement a significant direct influence of the applied stress on the SSA evolution was observed which is not captured by the model Eq. (4). The data is however too limited to investigate this effect in greater detail. Apart from that, Eq. (4) seems to be well suited for modeling the SSA change of new snow.

Densification and metamorphism of new snow

S. Schleef et al.

Title Page

Abstract

Introduction

Conclusions

References

Tables

Figures

◀

▶

◀

▶

Back

Close

Full Screen / Esc

Printer-friendly Version

Interactive Discussion



For most of our measurements, Eq. (7) seems to describe the densification reasonably well, even though only two fit parameters are involved. A remaining uncertainty comes from differences in crystal habit. The examples in Fig. 8 have shown that densification can easily differ by about 18 %, which can not be explained by the temperature difference alone. These differences in crystal habit and their influence on the densification rate are not captured by our analysis. It seems unlikely that SSA is a sufficient geometrical description of new snow type in the densification rate, as suggested by Eq. (7). We note however, that the crystal habit does not show an evident influence on the SSA evolution for samples with similar SSA values and different habits.

In common snowpack models the shape is empirically included in the dendricity parameter (Vionnet et al., 2012; Lehning et al., 2002). The inclusion of such a parameter seems to be crucial, even though it is not sufficiently exploited yet since new snow is commonly assigned the same dendricity, irrespective of the new snow type. To improve the understanding of new snow densification beyond Eq. (7) it seems important to replace also the dendricity by an objective microstructural parameter which captures differences in crystal habit or shape. A candidate might be the anisotropy parameter Q as pursued by Löwe et al. (2013); Calonne et al. (2014) to reduce the scatter in the data for the thermal conductivity. A direct application of the methods from Löwe et al. (2013) is however not possible, since the correlation function for new snow can certainly not be approximated by a simple exponential form. A potential generalization of the methods from Löwe et al. (2013), tailored to new snow, is left for future work.

5 Conclusions

We have shown that the rate of SSA decrease and thereby the SSA itself has probably the most dominant influence on isothermal new snow densification. It is inevitable that the assumption of isothermal conditions for the new snow deposit is only occasionally and approximately valid in nature. But given the experimental difficulties of both, characterizing the true thermal driving of the near surface snow in the field and reproducing

these conditions within tomography experiments, we believe that our isothermal experiments provide a valuable reference data set. For a quantitative characterization, we have derived a parametrization for the SSA decrease and densification rate which performs reasonably well for the entire data set of 45 time series (and a total of 600 μ CT measurements) of new snow experiments which were evaluated for the present analysis. Though advanced microstructural characteristics like the Euler number give additional insight in the interpretation of the densification experiments, it is likely that an additional shape parameter is required to reduce the remaining scatter in the description of new snow densification.

Supplementary material related to this article is available online at <http://www.the-cryosphere-discuss.net/8/1795/2014/tcd-8-1795-2014-supplement.zip>.

Acknowledgements. This work was funded by the Swiss National Science Foundation (SNSF) through Grant No. 200021_132549.

References

- Arnaud, L., Barnola, J. M., and Duval, P.: Physical modeling of the densification of snow/firn and ice in the upper part of polar ice sheets, in: Physics of Ice Core Records, vol. 159, edited by: Hondoh, T., Hokkaido University Press, Sapporo, Japan, 285–305, 2000. 1803
- Arnaud, L., Picard, G., Champollion, N., Dominé, F., Gallet, J.-C., Lefebvre, E., Fily, M., and Barnola, J. M.: Measurement of vertical profiles of snow specific surface area with a 1 cm resolution using infrared reflectance: instrument description and validation, *J. Glaciol.*, 57, 17–29, 2011. 1809
- Bader, H.: Theory of densification of dry snow on high polar glaciers, US Army SIPRE Res. Rep., US Army Corps of Engineers, Snow Ice and Permafrost Research Establishment (SIPRE), Wilmette, Illinois, 69, 1960. 1803

TCD

8, 1795–1829, 2014

Densification and metamorphism of new snow

S. Schleef et al.

Title Page

Abstract

Introduction

Conclusions

References

Tables

Figures

◀

▶

◀

▶

Back

Close

Full Screen / Esc

Printer-friendly Version

Interactive Discussion



Densification and metamorphism of new snow

S. Schleef et al.

Title Page

Abstract

Introduction

Conclusions

References

Tables

Figures

◀

▶

◀

▶

Back

Close

Full Screen / Esc

Printer-friendly Version

Interactive Discussion



Bartelt, P. and Lehning, M.: A physical SNOWPACK model for the Swiss avalanche warning Part I: numerical model, *Cold Reg. Sci. Technol.*, 35, 123–145, doi:10.1016/S0165-232X(02)00074-5, 2002. 1809

Cabanes, A., Legagneux, L., and Dominé, F.: Evolution of the specific surface area and of crystal morphology of Arctic fresh snow during the ALERT 2000 campaign, *Atmos. Environ.*, 36, 2767–2777, 2002. 1798

Cabanes, A., Legagneux, L., and Dominé, F.: Rate of evolution of the specific surface area of surface snow layers, *Environ. Sci. Technol.*, 37, 661–666, doi:10.1021/es025880r, 2003. 1798

Calonne, N., Flin, F., Geindreau, C., Lesaffre, B., and Rolland du Roscoat, S.: Study of a temperature gradient metamorphism of snow from 3-D images: time evolution of microstructures, physical properties and their associated anisotropy, *The Cryosphere Discuss.*, 8, 1407–1451, doi:10.5194/tcd-8-1407-2014, 2014. 1813

Carmagnola, C. M., Morin, S., Lafaysse, M., Domine, F., Lesaffre, B., Lejeune, Y., Picard, G., and Arnaud, L.: Implementation and evaluation of prognostic representations of the optical diameter of snow in the detailed snowpack model SURFEX/ISBA-Crocus, *The Cryosphere Discuss.*, 7, 4443–4500, doi:10.5194/tcd-7-4443-2013, 2013. 1797, 1809

Delmas, L.: Influence of snow type and temperature on snow viscosity, *J. Glaciol.*, 59, 87–92, doi:10.3189/2013JoG11J231, 2013. 1803

Dominé, F., Taillandier, A. S., and Simpson, W. R.: A parameterization of the specific surface area of seasonal snow for field use and for models of snowpack evolution, *J. Geophys. Res.*, 112, F02031, doi:10.1029/2006jf000512, 2007. 1798, 1802, 1811

Flanner, M. G. and Zender, C. S.: Linking snowpack microphysics and albedo evolution, *J. Geophys. Res.*, 111, D12208, doi:10.1029/2005jd006834, 2006. 1797, 1801, 1809

Gallet, J.-C., Domine, F., Zender, C. S., and Picard, G.: Measurement of the specific surface area of snow using infrared reflectance in an integrating sphere at 1310 and 1550 nm, *The Cryosphere*, 3, 167–182, doi:10.5194/tc-3-167-2009, 2009. 1809

Jordan, R.: A one-dimensional temperature model for a snow cover: technical documentation for SNTHERM.89, CRREL Spec. Rep., US Army Corps of Engineers, Cold Regions Research and Engineering Laboratory (CRREL), Hanover, New Hampshire, 91–16, 1991. 1797, 1809

Densification and metamorphism of new snow

S. Schleef et al.

Title Page

Abstract

Introduction

Conclusions

References

Tables

Figures

◀

▶

◀

▶

Back

Close

Full Screen / Esc

Printer-friendly Version

Interactive Discussion



- Kaempfer, T. and Schneebeli, M.: Observation of isothermal metamorphism of new snow and interpretation as a sintering process, *J. Geophys. Res.*, 112, D24101, doi:10.1029/2007JD009047, 2007. 1799, 1801
- Kikuchi, K., Kameda, T., Higuchi, K., and Yamashita, A.: A global classification of snow crystals, ice crystals, and solid precipitation based on observations from middle latitudes to polar regions, *Atmos. Res.*, 132–133, 460–472, 2013. 1805, 1819
- Kirchner, H. O. K., Michot, G., Narita, H., and Suzuki, T.: Snow as a foam of ice: plasticity, fracture and the brittle-to-ductile transition, *Philos. Mag. A*, 81, 2161–2181, 2001. 1803, 1807, 1811
- Kwon, Y., Thornton, K., and Voorhees, P.: Coarsening of bicontinuous structures via nonconserved and conserved dynamics, *Phys. Rev. E*, 75, 021120, doi:10.1103/PhysRevE.75.021120, 2007. 1802, 1812
- Legagneux, L. and Dominé, F.: A mean field model of the decrease of the specific surface area of dry snow during isothermal metamorphism, *J. Geophys. Res.*, 110, F04011, doi:10.1029/2004jf000181, 2005.
- Legagneux, L., Cabanes, A., and Dominé, F.: Measurement of the specific surface area of 176 snow samples using methane adsorption at 77 K, *J. Geophys. Res.*, 107, 4335, doi:10.1029/2001jd001016, 2002. 1802, 1811
- Legagneux, L., Lauzier, T., Dominé, F., Kuhs, W. F., Heinrichs, T., and Techmer, K.: Rate of decay of specific surface area of snow during isothermal experiments and morphological changes studied by scanning electron microscopy, *Can. J. Phys.*, 81, 459–468, doi:10.1139/p03-025, 2003. 1798
- Legagneux, L., Taillandier, A. S., and Dominé, F.: Grain growth theories and the isothermal evolution of the specific surface area of snow, *J. Appl. Phys.*, 95, 6175–6184, doi:10.1063/1.1710718, 2004. 1801, 1806, 1809, 1810
- Lehning, M., Bartelt, P., Brown, B., Fierz, C., and Satyawali, P.: A physical SNOWPACK model for the Swiss avalanche warning Part II. Snow microstructure, *Cold Reg. Sci. Technol.*, 35, 147–167, doi:10.1016/S0165-232X(02)00072-1, 2002. 1797, 1813
- Löwe, H., Spiegel, J., and Schneebeli, M.: Interfacial and structural relaxations of snow under isothermal conditions, *J. Glaciol.*, 57, 499–510, doi:10.3189/002214311796905569, 2011. 1810

Densification and metamorphism of new snow

S. Schleef et al.

Title Page

Abstract

Introduction

Conclusions

References

Tables

Figures

◀

▶

◀

▶

Back

Close

Full Screen / Esc

Printer-friendly Version

Interactive Discussion



- Löwe, H., Riche, F., and Schneebeli, M.: A general treatment of snow microstructure exemplified by an improved relation for thermal conductivity, *The Cryosphere*, 7, 1473–1480, doi:10.5194/tc-7-1473-2013, 2013. 1813
- Matzl, M. and Schneebeli, M.: Measuring specific surface area of snow by near-infrared photography, *J. Glaciol.*, 52, 558–564, 2006. 1809
- McCreight, J. L. and Small, E. E.: Modeling bulk density and snow water equivalent using daily snow depth observations., *The Cryosphere Discuss.*, 7, 5007–5049, doi:10.5194/tcd-7-5007-2013, 2013. 1797
- Michelsen, K., DeRaedt, H., and DeHosson, J.: Aspects of mathematical morphology, *Adv. Imag. Elect. Phys.*, 125, 119–194, 2003. 1800
- Perovich, D. K.: Light reflection and transmission by a temperate snow cover, *J. Glaciol.*, 53, 201–210, 2007. 1797
- Petrenko, V. F. and Whitworth, R. W.: *Physics of Ice*, Oxford University Press, Oxford, 1999. 1800, 1807, 1809
- Schleef, S. and Löwe, H.: X-ray microtomography analysis of isothermal densification of new snow under external mechanical stress, *J. Glaciol.*, 59, 233–243, doi:10.3189/2013JoG12J076, 2013. 1797, 1798, 1800, 1801, 1805, 1808, 1810, 1819, 1823
- Schleef, S., Jaggi, M., Löwe, H., and Schneebeli, M.: An improved machine to produce nature-identical snow in the laboratory, *J. Glaciol.*, 60, 94–102, doi:10.3189/2014JoG13J118, 2014a. 1799, 1801, 1810
- Schleef, S., Löwe, H., and Schneebeli, M.: Hot pressure sintering of low-density snow analyzed by X-ray microtomography and in-situ microcompression, *Acta Mater.*, in press, 2014b. 1798, 1800, 1807, 1812
- Steinkogler, W., Fierz, C., Lehning, M., and Obleitner, F.: Systematic Assessment of New Snow Settlement in SNOWPACK, *International Snow Science Workshop, Davos, Switzerland*, edited by: Schweizer, J. and VanHerwijnen, A., 27 September–2 October 2009, 132–135, 2009. 1796
- Taillandier, A. S., Dominé, F., Simpson, W. R., Sturm, M., and Douglas, T. A.: Rate of decrease of the specific surface area of dry snow: isothermal and temperature gradient conditions, *J. Geophys. Res.*, 112, F03003, doi:10.1029/2006jf000514, 2007. 1798
- Thompson, G., Field, P. R., Rasmussen, R. M., and Hall, W. D.: Explicit forecasts of winter precipitation using an improved bulk microphysics scheme. Part II: Implementation of a new snow parameterization, *Mon. Weather Rev.*, 136, 5095–5115, 2008. 1797

Vetter, R., Sigg, S., Singer, H. M., Kadau, D., Herrmann, H. J., and Schneebeli, M.: Simulating isothermal aging of snow, *EPL-Europhys. Lett.*, 89, 26001, doi:10.1209/0295-5075/89/26001, 2010. 1810

5 Vionnet, V., Brun, E., Morin, S., Boone, A., Faroux, S., Le Moigne, P., Martin, E., and Willemet, J.-M.: The detailed snowpack scheme Crocus and its implementation in SURFEX v7.2, *Geosci. Model Dev.*, 5, 773–791, doi:10.5194/gmd-5-773-2012, 2012. 1797, 1809, 1813

Densification and metamorphism of new snow

S. Schleef et al.

Title Page

Abstract

Introduction

Conclusions

References

Tables

Figures

⏪

⏩

◀

▶

Back

Close

Full Screen / Esc

Printer-friendly Version

Interactive Discussion



Densification and metamorphism of new snow

S. Schleef et al.

Table 1. Set IDs (1–8) correspond to natural snow while (9–14) are nature-identical snow samples. The sets 9 and 10 were already used in Schleef and Löwe (2013) and included here for comparison. For each set the number of samples N_s and the total number of measurements N_m from the time series are given in addition to applied stresses σ and used temperatures T . The initial values of ice fraction $\overline{\phi}_{\text{ice},0}$ and specific surface area $\overline{\text{SSA}}_0$ are averages over all samples within the set. For all observed crystal habits the classification number is given according to Kikuchi et al. (2013), including potentially broken parts (I3a) of them.

Snow ID	N_s	N_m	σ Pa	T °C	$\overline{\phi}_{\text{ice},0}$	$\overline{\text{SSA}}_0$ mm ⁻¹	Class. No.
1	2	32	133, 215	-18	0.08	92	P3a, P3b, R1c, H1a, I2a
2	5	76	0, 133, 215, 318	-18	0.11	64	P2b, P4c, P4d
3	7	90	0, 133, 215, 318	-18	0.07	102	P3a, R1c, I2a
4	4	43	0, 133, 215, 318	-18	0.08	91	P3b, R1c
5	2	68	0	-13	0.11	77	C3b, C3c, C4d, P3a, P3b, A1a
6	2	30	0	-13	0.09	75	P3b, P4e, P4f, A2a, R1c
7	2	24	0	-13	0.08	92	C4b, C4d, P2b, H1a, H1b
8	2	24	0	-13	0.06	86	P1a, P2a, P3a, P3b, P4e, P4g
9	7	111	0, 133, 215, 318	-18	0.11	66	not analyzed
10	2	32	215	-18	0.10	69	not analyzed
11	1	19	0	-13	0.07	74	P3b, P3c, P4c
12	2	23	0	-13	0.07	75	P3b, P3c
13	1	8	0	-13	0.12	66	C1a, C1b, C1c, I1a
14	6	48	0, 133	-3, -8, -13	0.08	74	P3b, P3c

[Title Page](#)
[Abstract](#)
[Introduction](#)
[Conclusions](#)
[References](#)
[Tables](#)
[Figures](#)
[◀](#)
[▶](#)
[◀](#)
[▶](#)
[Back](#)
[Close](#)
[Full Screen / Esc](#)
[Printer-friendly Version](#)
[Interactive Discussion](#)


Densification and metamorphism of new snow

S. Schleef et al.

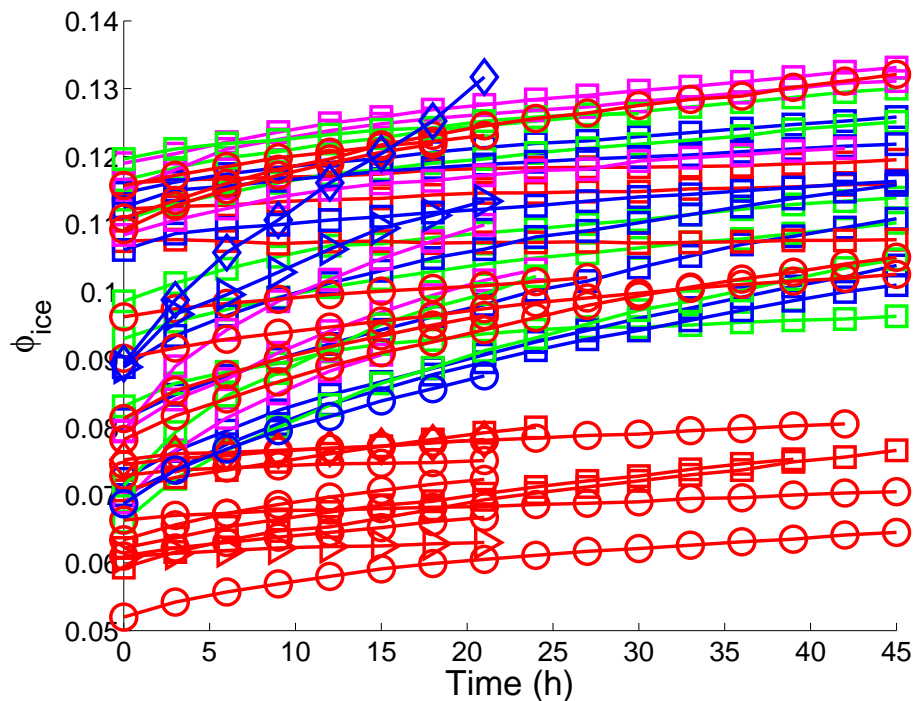


Fig. 1. Evolution of the ice volume fraction ϕ_{ice} for all samples. The color of the symbols indicate different stress values (red: 0 Pa, blue: 133 Pa, green: 215 Pa, magenta: 318 Pa) and the temperature is encoded by different symbols (\square : -18°C , \circ : -13°C , \triangleright : -8°C , \diamond : -3°C).

Title Page

Abstract

Introduction

Conclusions

References

Tables

Figures

◀

▶

◀

▶

Back

Close

Full Screen / Esc

Printer-friendly Version

Interactive Discussion



Densification and metamorphism of new snow

S. Schleef et al.

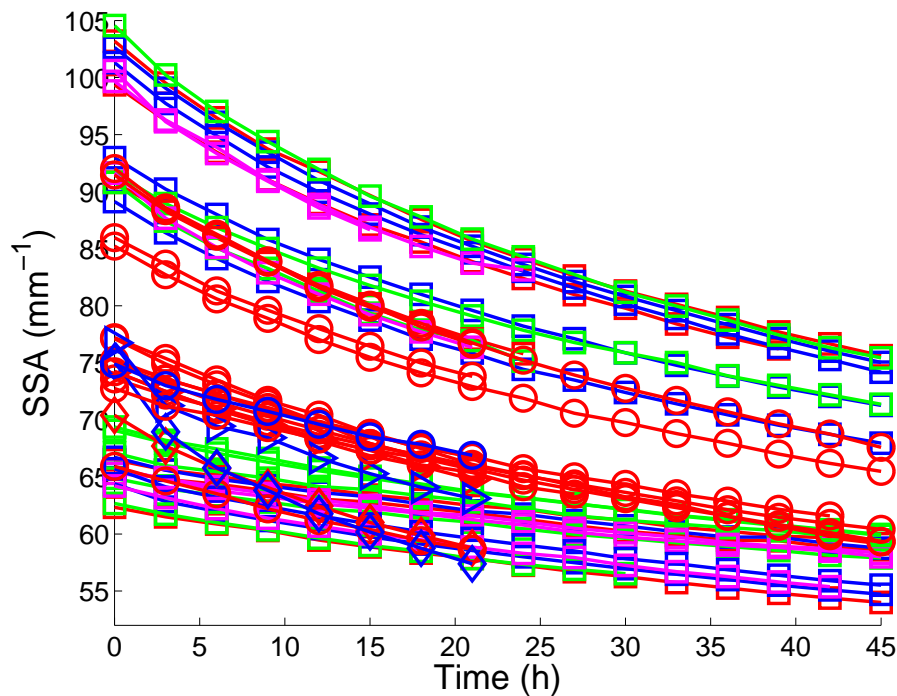


Fig. 2. Evolution of the SSA for all samples. The color of the symbols indicate different stress values (red: 0 Pa, blue: 133 Pa, green: 215 Pa, magenta: 318 Pa) and the temperature is encoded by symbols (□: -18 °C, ○: -13 °C, ▵: -8 °C, ◇: -3 °C).

Title Page

Abstract

Introduction

Conclusions

References

Tables

Figures

◀

▶

◀

▶

Back

Close

Full Screen / Esc

Printer-friendly Version

Interactive Discussion



Densification and metamorphism of new snow

S. Schleef et al.

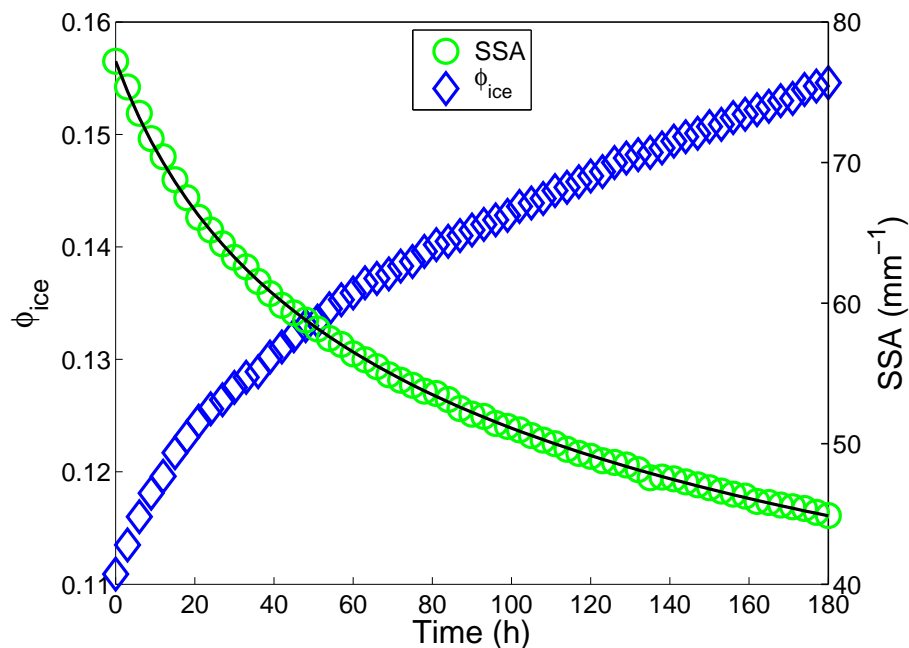


Fig. 3. Evolution of ice fraction and SSA in one week at about -13°C . The initial structure and crystal habit of this natural snow sample are shown in Fig. 8 bottom and listed as snow 5 in Table 1. A fit for the SSA according to Eq. (1) is plotted as black line.

[Title Page](#)[Abstract](#)[Introduction](#)[Conclusions](#)[References](#)[Tables](#)[Figures](#)[◀](#)[▶](#)[◀](#)[▶](#)[Back](#)[Close](#)[Full Screen / Esc](#)[Printer-friendly Version](#)[Interactive Discussion](#)

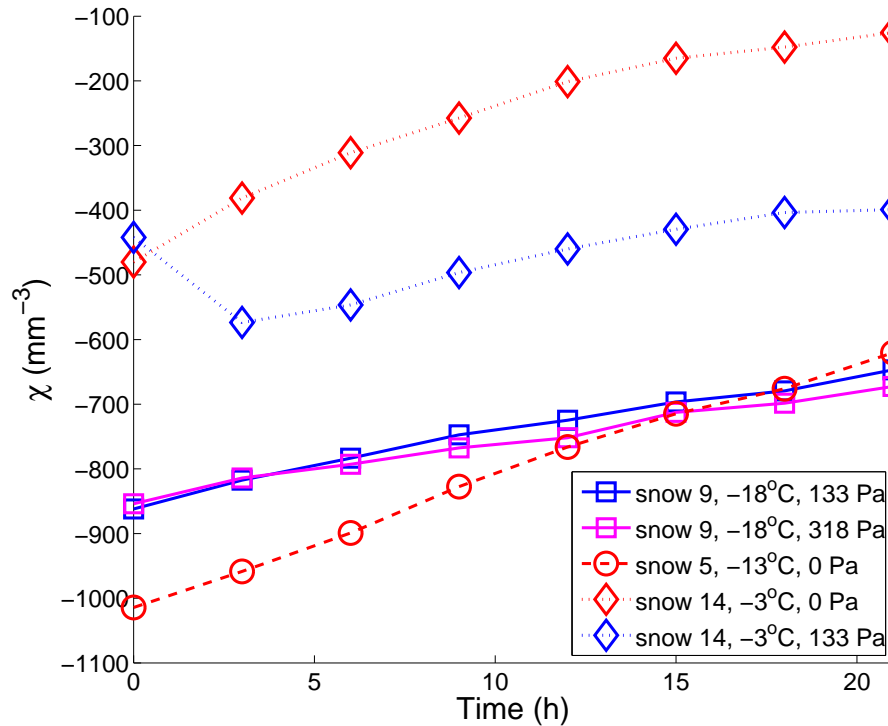


Fig. 4. Examples of the evolution of the Euler characteristic χ for different new snow types (cf. Table 1) during the first day of settlement. The sample of the week measurement (snow 5, Fig. 3), two examples of snow 9 with different applied stresses belonging to the experiments presented by Schleef and Löwe (2013), and two examples of snow 14 with different applied stresses at -3°C , are shown.

Densification and metamorphism of new snow

S. Schleef et al.

Title Page

Abstract Introduction

Conclusions References

Tables Figures

◀ ▶

◀ ▶

Back Close

Full Screen / Esc

Printer-friendly Version

Interactive Discussion



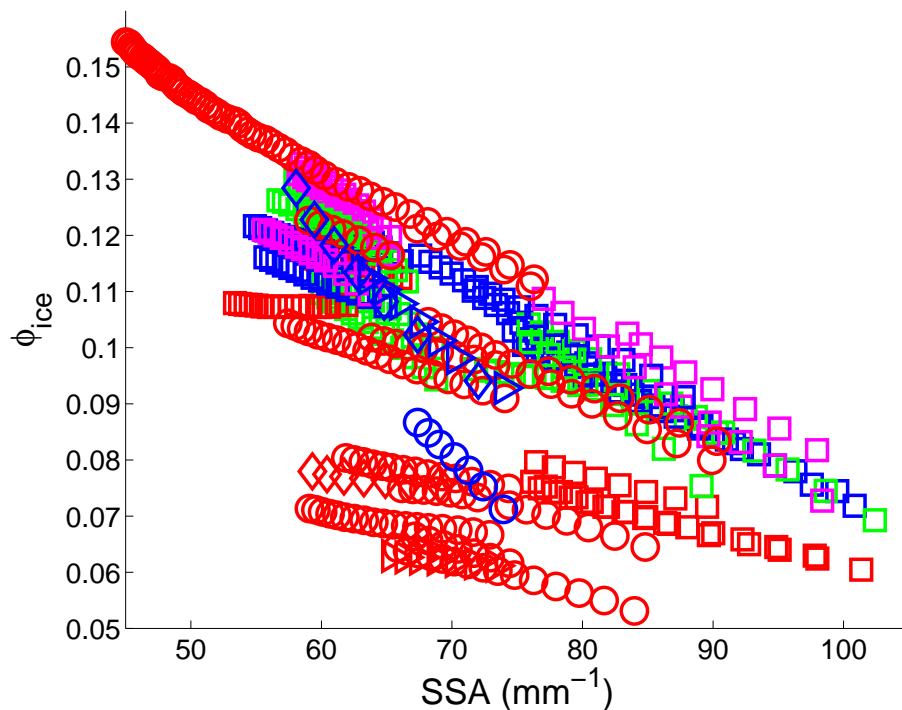


Fig. 5. Comparison between the evolution of the ice fraction and the specific surface area of our complete data showing an almost linear relation for each series of measurement. Legend: stress indicated by colors: red: 0 Pa, blue: 133 Pa, green: 215 Pa, magenta: 318 Pa; temperature indicated by symbols: \square : -18°C , \circ : -13°C , \triangleright : -8°C , \diamond : -3°C ; snow types are indistinguishable.

Densification and metamorphism of new snow

S. Schleef et al.

Title Page	
Abstract	Introduction
Conclusions	References
Tables	Figures
◀	▶
◀	▶
Back	Close
Full Screen / Esc	
Printer-friendly Version	
Interactive Discussion	



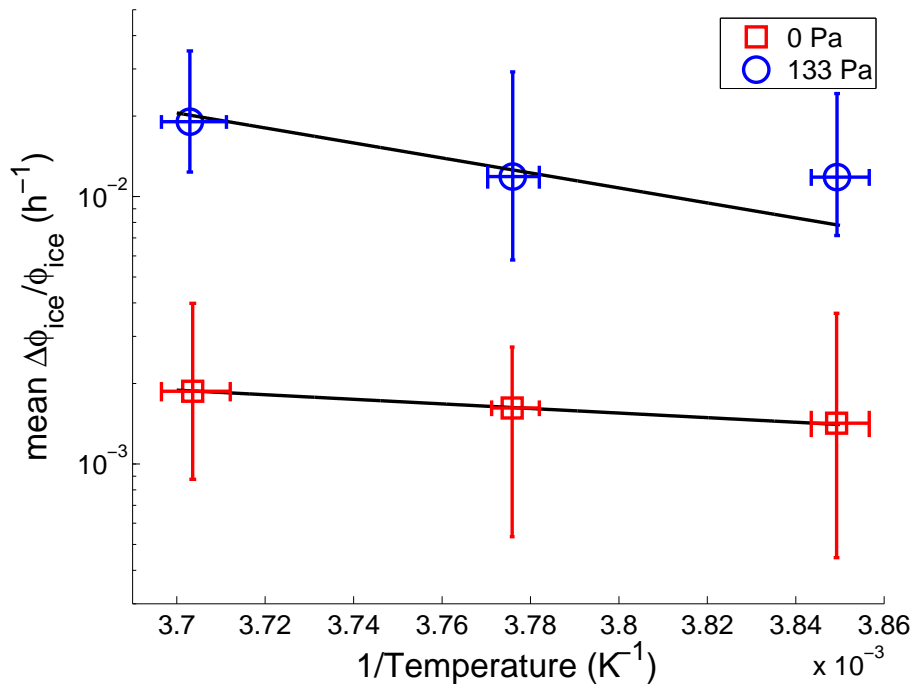


Fig. 6. Mean densification rate for experiments at different temperatures.

Title Page

Abstract Introduction

Conclusions References

Tables Figures

◀ ▶

◀ ▶

Back Close

Full Screen / Esc

Printer-friendly Version

Interactive Discussion



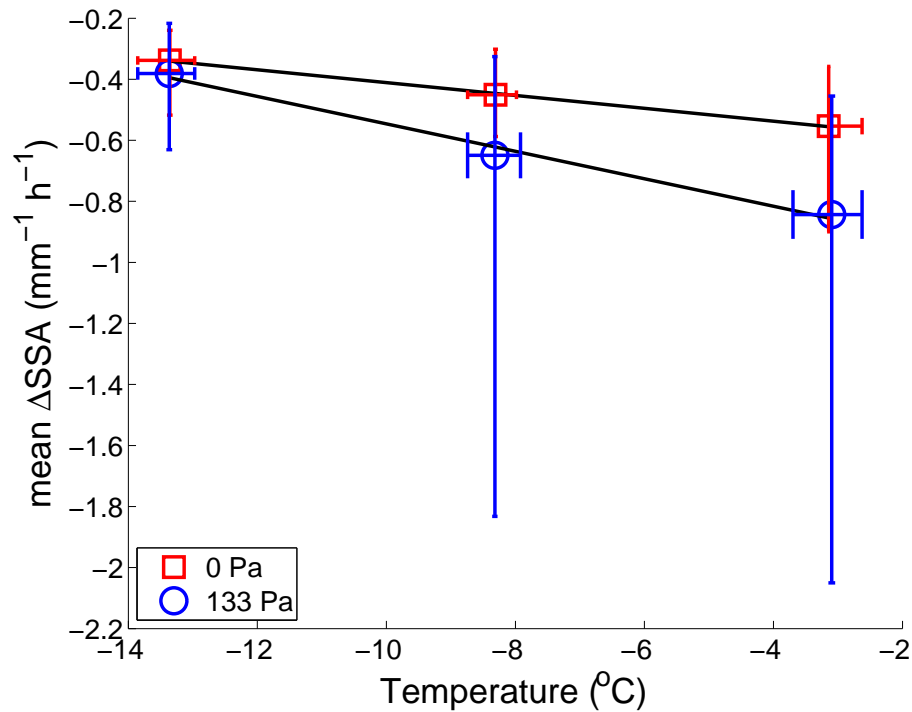


Fig. 7. Mean SSA decay for experiments at different temperatures.

Densification and metamorphism of new snow

S. Schleef et al.

Title Page

Abstract Introduction

Conclusions References

Tables Figures

◀ ▶

◀ ▶

Back Close

Full Screen / Esc

Printer-friendly Version

Interactive Discussion



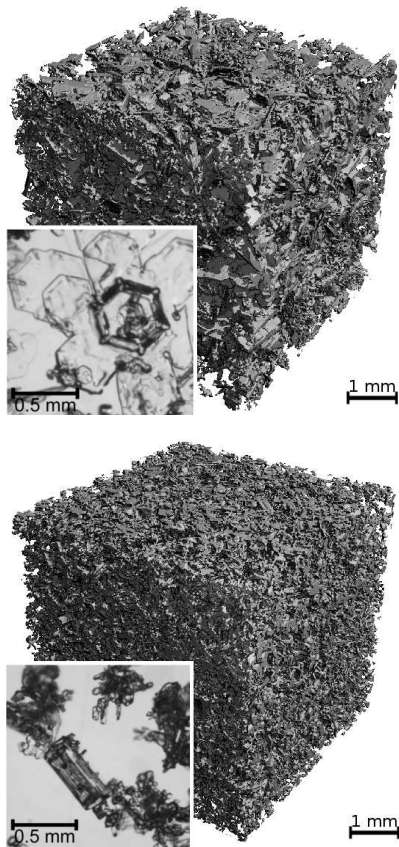


Fig. 8. Examples of natural snow samples with a photograph of the exemplary crystal habit and an μ CT image of the initial structure. The parameters of the sample at top are $\phi_{\text{ice},0} \approx 0.1$ and $\text{SSA}_0 \approx 62 \text{ mm}^{-1}$ (snow 2 in Table 1), and of the sample at bottom $\phi_{\text{ice},0} \approx 0.1$ and $\text{SSA}_0 \approx 77 \text{ mm}^{-1}$ (snow 5 in Table 1, evolution shown in Fig. 3).

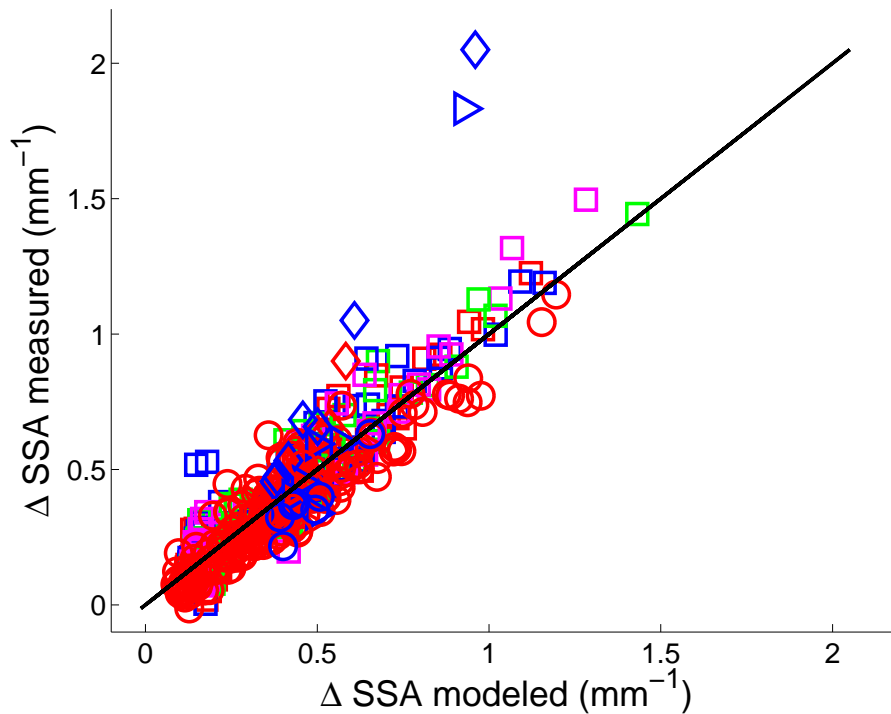


Fig. 9. Modeled SSA change according to Eq. (4) vs. measuring results. Legend: stress indicated by colors: red: 0 Pa, blue: 133 Pa, green: 215 Pa, magenta: 318 Pa; temperature indicated by symbols: \square : -18°C , \circ : -13°C , \triangleright : -8°C , \diamond : -3°C ; snow types are indistinguishable.

Densification and metamorphism of new snow

S. Schleef et al.

Title Page	
Abstract	Introduction
Conclusions	References
Tables	Figures
◀	▶
◀	▶
Back	Close
Full Screen / Esc	
Printer-friendly Version	
Interactive Discussion	



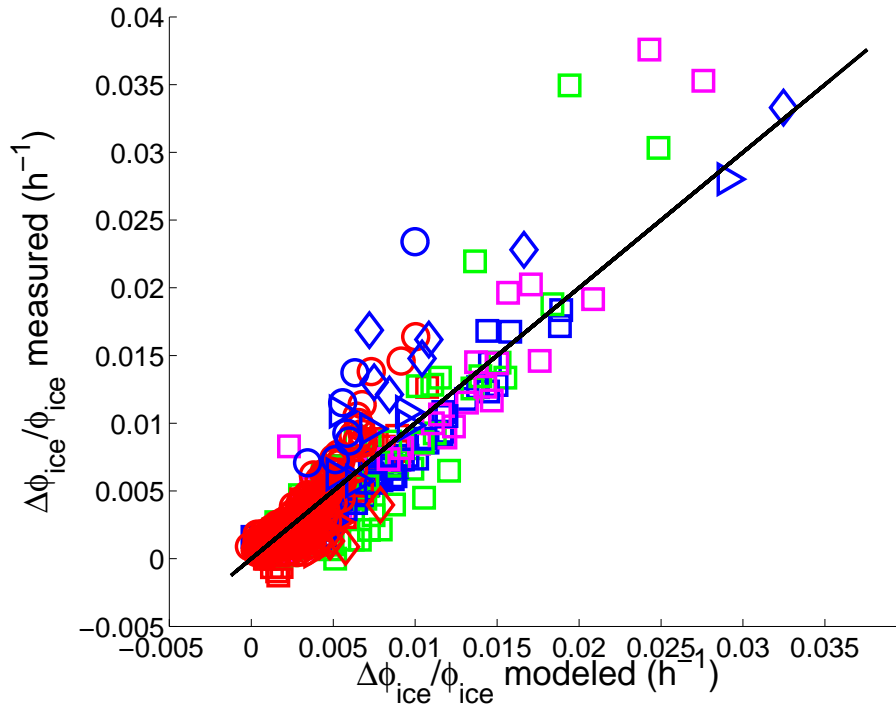


Fig. 10. Modeled $\dot{\phi}/\phi$ according to Eq. (7) vs. measuring results. Legend: stress indicated by colors: red: 0 Pa, blue: 133 Pa, green: 215 Pa, magenta: 318 Pa; temperature indicated by symbols: \square : -18°C , \circ : -13°C , \triangleright : -8°C , \diamond : -3°C ; snow types are indistinguishable.

Densification and metamorphism of new snow

S. Schleef et al.

Title Page	
Abstract	Introduction
Conclusions	References
Tables	Figures
◀	▶
◀	▶
Back	Close
Full Screen / Esc	
Printer-friendly Version	
Interactive Discussion	

